Received: May 8, 2022. Revised: June 14, 2022.

International Journal of
Intelligent Engineering & Systems

http://www.inass.org/

Conception and Hardware Implementation of MPPT Controller for Partially Shaded Photovoltaic Panels using Backstepping and Neural Network based Particle Swarm Optimization

Khalid Chennoufi[1]* **Mohammed Ferfra[1]** **Hicham Bouzakri[1]**

[1]*Department of Electrical Engineering, Mohammadia School of Engineers, Mohammed V University in Rabat, Morocco*
* Corresponding author's Email: khalidchennoufi@research.emi.ac.ma

Abstract: In this paper, in order to track the maximum power point under partial shading condition, An Artificial Neural Network based Particle Swarm Optimization (ANNPSO) combined with backstepping controller has been employed. The proposed controller relay to the ability of the PSO to find the global maximum power point and to the ANN to generate a reference voltage according to the PSO data without oscillations. The backstepping controller has been employed in order to track the reference voltage generated by the ANN by adjusting the duty cycle of the SEPIC converter. The simulation was carried out using MATLAB software. On one hand, the results affirms the ability of the proposed controller to find and to track the global maximum power point, and on the other hand the present method demonstrates high efficiency against previous works, The results shows that the proposed method tracks the reference voltage within 20 ms and it is able to tracks the GMPP with high performance. Furthermore, the experimental study shows that the proposed controller can be easily implemented using low coast materials, and the obtained results show a gain of 5W compared to the controller that combine the incremental conductance with backstepping.

Keywords: Photovoltaic array, Partial shading, Artificial neural network, Particle swarm optimization, Backstepping.

Nomenclature

PV	: photovoltaic	V_m	: maximum voltage
PSO	: particle swarm optimization	I_m	: maximum current
ANN	: Artificial neural network	V_{co}	: open-circuit voltage
BSC	: Backstepping control	I_{cc}	: short-circuit voltage
SMC	: Sliding mode control	K_i	: temperature coefficient of short-circuit current
InC	: incremental conductance	K_v	: temperature coefficient of open-circuit voltage
P&O	: Perturb and Observe	a_1, a_2	: ideality factors
LMPP	: local maximum power point	I_{01}, I_{02}	: saturation currents
GMPP	: global maximum power point	Iph	: photocurrent
L_1, L_2	: SEPIC Inductors	R_s, R_p	: series and parallel resistances
C_1, C_2, C_3	: SEPIC capacitors	a_1, a_2	: ideality factors
V_{C2}	: voltage across second capacitor	I_{01}, I_{02}	: saturation currents
V_O	: output voltage	I_{ph}	: photocurrent
I_{L1} I_{L2}	: current through the 1st inductor and 2st inductor	e_1, e_2	: tracking errors
R	: Load	K_1, K_2	: positive constants
u	: Duty cycle	V_1, V_2	: Lyapunov functions

1. Introduction

The production of the photovoltaic array depends on several factors, such as wind, humidity, temperature and solar insolation [1]. However, another factor that influences the efficiency of the photovoltaic array and yields an important loss of the output power is the partial shading [1]. In partial shading condition the PV modules of the PV array are subjected to a non-uniform insolation, in this case the P-V curve shows a multiple peak [2], which correspond to local and global maximum powers instead of one maximum power in the case of uniform insolation. In the literature several MPPT algorithms have been proposed in the literature the most used are the conventional algorithms such as: Perturb and Observe (P&O) [3], incremental conductance (Inc) [4] and fractional open circuit voltage [5], these methods are simple and easy to implement but they suffer from fluctuation in addition they can't localise the global maximum power which can lead to a loss of power [6]. In order to improve the tracking efficiency the conventional algorithms are combined with nonlinear controller such as backstepping and sliding mode. In [7], the authors try to limit the chattering phenomena of sliding mode and to reduce the oscillations of perturb and observe loop. The proposed method which combines the two algorithms exhibits good convergence speed, but the main disadvantage is the oscillations remain around the maximum power point and the proposed algorithm. In [8], the authors propose a hybrid MPPT which combines incremental conductance with backstepping controller, the results shows that the proposed algorithm tracks the reference voltage whit small oscillations. The hybrid method exhibits their superiority to the conventional methods. However, they suffer from the same drawback of the conventional algorithms, as they fail to track the global maximum power in partial shading condition. Recently, several technics based on the optimisation algorithms have been proposed in the literature, such as Particle Swarm Optimization (PSO) [9], Differential Evolution algorithm (DE) [10] and Genetic Algorithm (GA) [11], these algorithms have the advantage of localising and tracking the global maximum power point, however, they suffer from fluctuation around the steady state and specially when the environmental condition change [12]. In order to improve the tracking procedure under partial shading, [13] has presented a combination between the PSO and sliding mode control. In this algorithm the PSO was designed to generate the reference voltage, while the sliding mode has been conceived to track the generated voltage. An improved MPPT controller under partial shading has been presented by [14], which consist of a combination between a new loop entitled SLG and backstepping controller. The SLG sweeps the PV curve, looks for the global maximum power point, and generates the reference voltage, while the backstepping controller tracks this latter by adjusting the duty cycle of the converter. Although the proposed algorithms track the maximum power point under partial shading, it can be seen that the osculation at brusque variation of the environmental condition is the main drawback of these approaches. In this work, a combination between Artificial Neural Network based Particle Swarm Optimization (ANNPSO) with backstepping controller is proposed. The aim is to provide a MPPT controller capable to track the global maximum power point under partial shading without high efficiency. The (ANNPSO) is conceived by training the Artificial Neural Network with PSO data using different shading scenarios, the ANN has been designed with two entrée, current and temperature, and one output which correspond to the voltage at the global maximum power point. The role of the backstepping controller is to track the reference voltage generated by the ANN, the present work adopts double diode model for an accurate modelling and in order to have a fast and stable tracking the single-ended primary converter has been employed.

The present paper is structured as follows. In Section 2, the modelling of the PV system is presented. The controller was developed in section 3. The simulation and discussion are illustrated in Section 4. The experimental study is shown in the Section 5.

2. Modelling of the PV system

The photovoltaic system considered in this work consists of a PV array of SUNPRO module, Single Ended Primary Inductor Converter (SEPIC) connected to a resistive load, and a Maximum Power Point controller, as shown in Fig. 1.

2.1 Modeling of the SEPIC converter

The single-ended primary inductor converter is a DC-DC converter which can makes the voltage greater than, less than, or equal to the voltage input. The architecture of the SEPIC converter consists of a boost converter followed by an inverted buck-boost converter, which allows tracking the maximum power point with low current ripples [15]

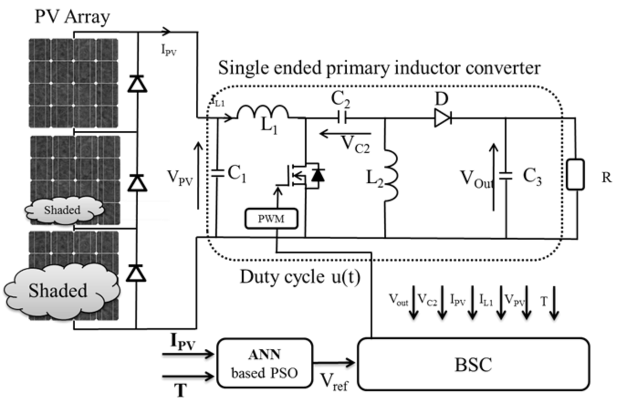

Figure. 1 Schematic of the proposed PV system

with a non-inverted output [16]. The converter is modelled mathematically by a combination between the stat space when the switch is on and when it's off [17], which can be expressed by the following equations:

$$\frac{dI_{L1}}{dt} = \frac{(u-1)V_{C2}}{L_1} + \frac{(u-1)V_o}{L_1} + \frac{V_{PV}}{L_1} \quad (1)$$

$$\frac{dV_{C2}}{dt} = \frac{(1-u)I_{L1}}{C_2} + \frac{dI_{L2}}{C_2} \quad (2)$$

$$\frac{dI_{L2}}{dt} = -\frac{dV_{C2}}{L_2} + \frac{(1-u)V_o}{L_2} \quad (3)$$

$$\frac{dV_O}{dt} = \frac{(1-u)I_{L1}}{C_3} + \frac{(u-1)I_{L2}}{C_3} - \frac{V_O}{RC_3} \quad (4)$$

2.2 Modeling of photovoltaic module

The single diode model is commonly used in photovoltaic modelling because of its simplicity, since the recombination current is neglected [18]. However, it has been reported that the accuracy is not its strong point, as the errors between the simulated and experimental data are relatively high. Therefore, in this paper the junction recombination is modelled by adding a second diode, thus the photovoltaic panel is modelled based on the double diode model, as shown in Fig. 2.

The output current of a solar module is represented by:

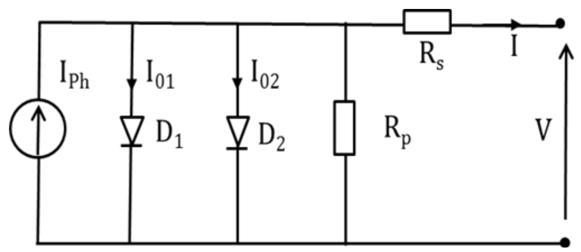

Figure. 2 Equivalent circuit of the double diode model

Table 1. Datasheet of the module SP 30 W

Parameters	Values
V_m (V)	17.3
I_m (A)	1.74
V_{co} (V)	21.7
I_{cc} (A)	1.89
K_i (A /K)	$0.35.10^{-3}$
K_v (V/K)	-0.100

Table 2. Extracted parameters of the module SP 30 W

Parameters	Values
a_1	1.0058
a_2	1.9941
I_{ph} (A)	1.8934
I_{01} (A)	1.0546×10^{-10}
I_{02} (A)	1.7469×10^{-05}
R_p (Ω)	468.2654
R_s (Ω)	0.8459

$$I_{PV} = I_{ph} - I_{01}\left(\exp\left(\frac{V+R_sI}{a_1V_T}\right) - 1\right) - I_{02}\left(\exp\left(\frac{V+R_sI}{a_2V_T}\right) - 1\right) - \frac{V+R_sI}{R_p} \quad (5)$$

The parameters a_1, a_2, I_{01}, I_{02}, I_{ph}, R_s and R_p are essential for the photovoltaic modelling. However, there are not given in the manufacturer datasheet, thus they are extracted using a combination between analytical and numerical methods as explained in [19]. The datasheet parameters of the module SP 30W are shown in the Table 1 and the extracted parameters are illustrated in Table 2.

3. Controller design

This section presents the design of the proposed controller, which consists of a combination between Artificial Neural Network based Particle Swarm Optimization (ANNPSO) and backstepping controller (BSC). ANN is designed to generate a reference voltage for each solar irradiation and temperature which corresponds to the voltage of the global maximum power point. The BSC is developed to track the generated reference by adjusting the duty cycle of the SEPIC converter.

3.1 Design of the ANNPSO

The Artificial neural network (ANN) is a computing structure inspired by biological neural networks [20], it has been used for a wide range of applications, and among these applications is its implementation in the Maximum Power Point algorithms. In this work, the neural network was constructed and trained in neural network toolbox using Bayesian Regularization training algorithm, based on Particle Swarm Optimization algorithm.

The PSO has two main operators which are speed and position. It uses several particles or agents to find the maximum or minimum values of a function [21]. Each of the agents' moves in a given search space with a speed, (k). Then, a new velocity value for each agent is calculated based on the current velocity, the previous best position, and the overall best position for each iteration. Afterwards, the new position is updated using the previous position and the new speed value. The speed and position of the agents will be updated according to the following equations [22]:

$$v_i(k+1) = wv_i(k) + c_1r_1(p_{best,i} - s_i(k)) + c_2r_2(g_{best} - s_i(k)) \quad (6)$$

$$s_i(k+1) = s_i(k) + v_i(k+1) \quad (7)$$

Where:
$v_i(k)$: Vector of the current speed.
$v_i(k+1)$: Vector of the modified speed.
$s_i(k)$: Vector of the current position.
$s_i(k+1)$: Vector of the modified position.
w: inertia weight.
$p_{best,i}$: Best position found by a particle i.
g_{best}: Best position found by a group of particles.
c_1: Cognitive coefficient.
c_2: Social coefficient.
r_1: Random parameter, [0,1].
r_2: Random parameter, [0,1].

The flow chart of the PSO algorithm is illustrated in the Fig. 3.

In order to simulate the effect of partial shading a simulation has been performed in Matlab software using three PV modules of SUNPRO connected in series. These modules are considered to operate in partial shading condition, thus the solar insolation was considered to be not uniform for the three modules by varying the irradiance from 200 to 1000 W/m² for every module, in addition the temperature was increased from 280 to 320 Kelvin to simulate the true behaviour of the PV array in the outdoor conditions. The Global Maximum Power Point has been obtained using PSO algorithm combined with backstepping controller, a database was created by storing the reference voltage, the current and the temperature for each operating point. The Artificial Neural Network has been trained based on the obtained data in which the input was designed with two entries that correspond to the current and temperature while the output was designed with one neuron which correspond to the voltage at the global maximum power point. The figure 4 shows the regression fit, if the R values is higher than 0.93, the fit is considered good for all data sets, as can be seen the results illustrates an excellent fit, thus the ANN is validated and exhibits high performance.

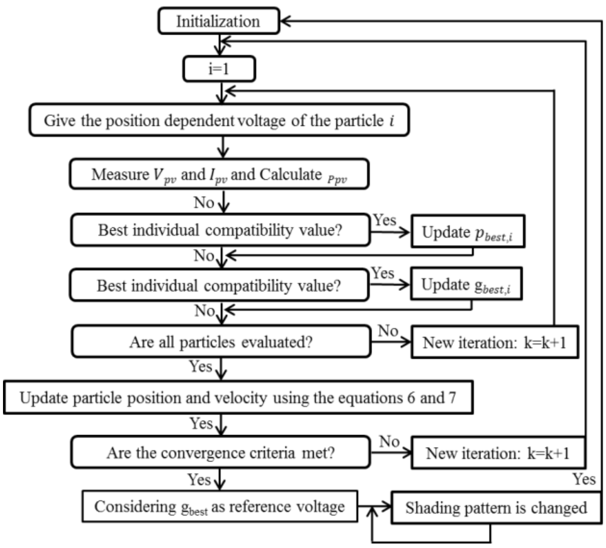

Figure. 3 Flow chart of the PSO algorithm

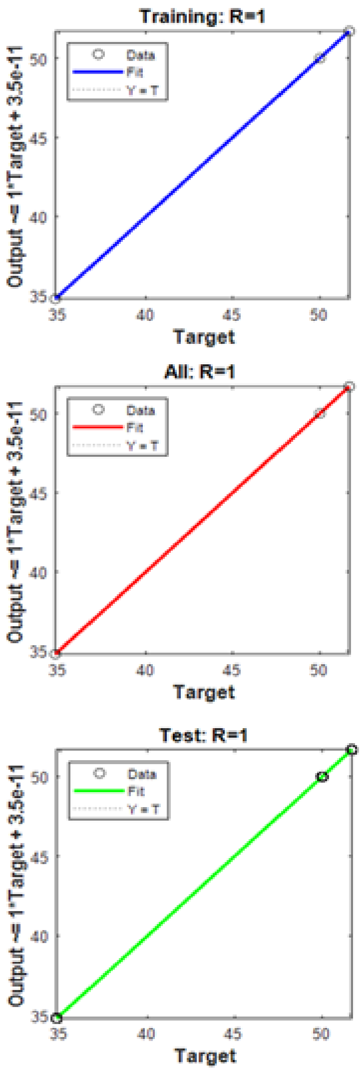

Figure. 4 ANN regression fit

3.2 Design of the BSC:

The BSC is designed to follow the estimated voltage by adjusting the duty cycle of the converter. The design of the controller is carried out by developing a control law based on a Lyapunov analysis.

Firstly, the voltage tracking error is defined as:

$$e_1 = V_{pv} - V_{ref} \tag{8}$$

Where:
V_{PV}: is the photovoltaic voltage
$V_{ref:}$ the reference voltage generated by the ANN

The Lyapunov function is introduced as follow:

$$V_1 = \frac{1}{2} e_1^2 \tag{9}$$

The derivative of Eq. (9) with respect to time is:

$$\dot{V}_1 = e_1 (\dot{V}_{pv} - \dot{V}_{ref}) \tag{10}$$

The Lyapunov function has to be negative definite derivative, the following equation is considered:

$$\dot{V}_1 = -K_1 e_1^2 \tag{11}$$

Consequently:

$$(\dot{V}_{pv} - \dot{V}_{ref}) = -K_1 e_1 \tag{12}$$

The photovoltaic current is given by:

$$I_{PV} = I_{C1} + I_{L1} \tag{13}$$

The derivative of photovoltaic tension can be written as:

$$\dot{V}_{pv} = \frac{I_{PV} - I_{L1}}{C_1} \tag{14}$$

The control law which corresponds to the desired current is:

$$I_d = I_{PV} + C_1 (K_1 e_1 - \dot{V}_{ref}) \tag{15}$$

Secondly, the error between the first inductor current and the desired current is introduced as:

$$e_2 = I_{L1} - I_d \tag{16}$$

The derivative of Lyapunov function with respect to the time can be expressed as:

$$\dot{V}_1 = e_1 \left[\left(\frac{I_{PV} - (e_2 + I_d)}{C_1} - \dot{V}_{ref} \right) \right] \tag{17}$$

By using Eqs. (12) and (14) the above equation can be written as:

$$\dot{V}_1 = -k_1 e_1^2 - \frac{e_1 e_2}{C_1} \tag{18}$$

The time derivative of (16), using the Eq. (1) can be written as:

$$\dot{I}_{PV} = \frac{dI_{PV}}{dV_{PV}} \frac{dV_{PV}}{dt} \tag{19}$$

By differentiating the Eq. (5) with respect to the voltage, the derivative of the photovoltaic current is obtained:

$$\dot{I}_{PV} = \left[-\frac{I_{01} exp\left(\frac{V + R_S I_{PV}}{a_1 V_T}\right)}{a_1 V_T} - \frac{I_{02} exp\left(\frac{V + R_S I_{PV}}{a_2 V_T}\right)}{a_2 V_T} - \frac{1}{R_P} \right] \dot{V}_{PV} \tag{20}$$

In order to guarantee the asymptotic stability of the system and the convergence of the errors e_1 and e_2 to zero, a composite Lyapunov function V_2 is defined as:

$$V_2 = V_1 + \frac{1}{2} e_2^2 \tag{21}$$

The derivative of V_2 with respect to the time is:

$$\dot{V}_2 = \dot{V}_1 + e_2 \dot{e}_2 \tag{22}$$

By using Eq. (18) the derivative of V_2 can be expressed as:

$$\dot{V}_2 = -K_1 e_1^2 + e_2 \left[\frac{1}{L_1} V_{pv} - \frac{1}{L_1} (1 - u)(V_{out} + V_{c2}) - \dot{I}_d - \frac{e_1}{C_1} \right] \tag{23}$$

The time derivative of Lyapunov function has to be negative definite:

$$\frac{1}{L_1} V_{pv} - \frac{1}{L_1} (1 - u)(V_{out} + V_{c2}) - \dot{I}_d - \frac{e_1}{C_1} = -K_2 e_2 \tag{24}$$

Where K_2 is a positive constant.

The control law, which guarantees e_1, e_2 converges asymptotically to 0, is given by:

$$u = 1 - \left[V_{PV} + L_1 \left(K_2 e_2 - \frac{e_1}{C_1} - \dot{I}_d \right) \right] \frac{1}{V_{C2} + V_0} \tag{25}$$

Received: May 8, 2022. Revised: June 14, 2022.

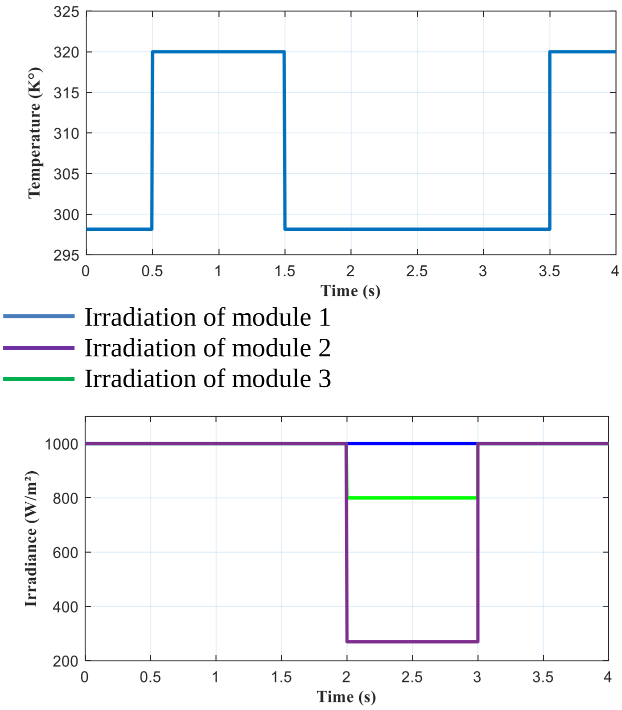

Figure. 5 Meteorological conditions

4. Simulation results

The photovoltaic array presented in this study consists of combination of three modules of SUNPRO 30 W. the simulation has been performed in MATLAB/simulink environment, in which the proposed controller has been evaluated in different meteorological condition as illustrated in the Fig. 5.

In the first interval, [0 - 2s], the three modules are considered operating in a uniform insolation which is 1000 W/m². During the second interval, [2s - 3s], in order to simulate the partial shading condition the photovoltaic array is subjected to a non-uniform insolation, hence the insolation of the module 1 has been maintained at 1000 w/m² while the insolation for the module 2 and 3 has been dropped to 800 W/m² and 270 W/m² respectively. In the last interval [3s - 4s] the insolation of the module 2 and 3 increase suddenly to reach 1000 W/m², thus the array is returned to operates in a uniform insolation. In regard of temperature, in increased to reach 298.15 K in the interval [0 - 0.5s] and [1.5s - 3.5s] and considered to be 320 K in the interval [0.5s-1.5s] and [3.5s-4s]. The simulation parameters are presented in the Table 3.

The Fig. 6 illustrates the photovoltaic current, voltage and power using different MPPT technics, which are the proposed method (ANNPSO-BSC) and compared to PSO-BSC, InC-BSC and to SLG-BSC, proposed by [8] and [13]. The results show that although all the method track successfully the reference voltage when the array are subjected to

Table 3. Simulation parameters

Parameter		Value
L_1 (mH)		0.35
L_2 (mH)		0.35
C_1 (μF)		440
C_2 (μF)		440
C_3 (μF)		1500
K_1		437
K_2		206
R(Ω)		150
Diode	Resistance Ron (Ω)	0.001
	Forwarded voltage (V)	0.8
	Snubber resistance Rs (Ω)	500
	Snubber capacitance Cs (F)	2.5×10^{-7}
IGBT	Resistance Ron (Ω)	0.001
	Forwarded voltage (V)	1
	Snubber resistance Rs (Ω)	10^5
	Snubber capacitance Cs (F)	inf

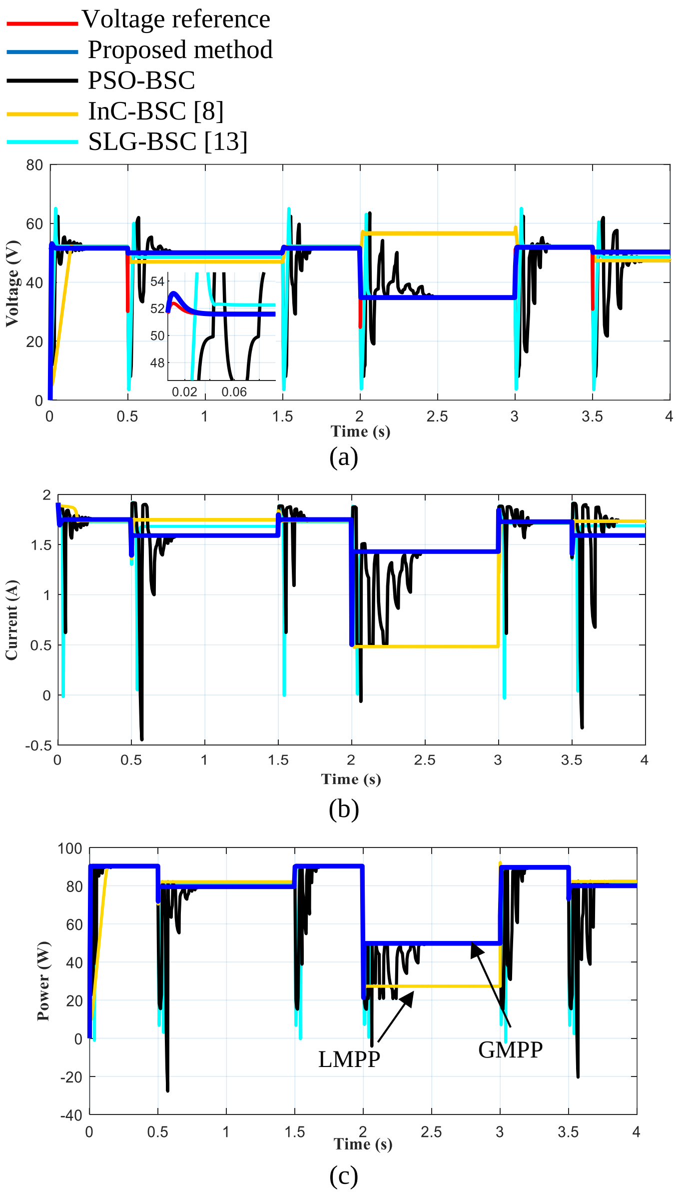

Figure. 6 Photovoltaic: (a) Voltage, (b) Current, and (c) Power

Received: May 8, 2022. Revised: June 14, 2022.

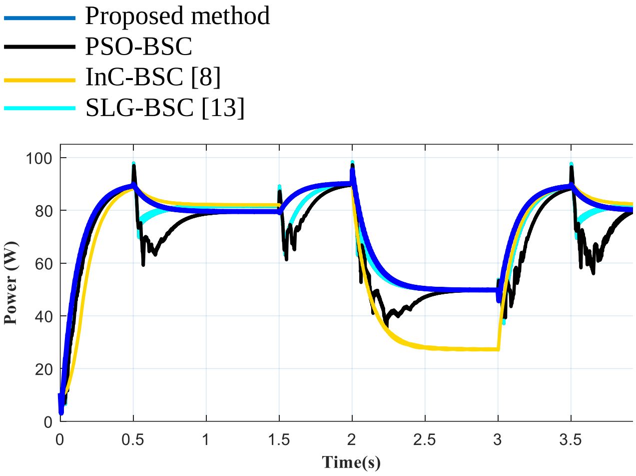

Figure. 7 Output power

uniform insolation, the proposed method present the fast and the stable response, as it reach the reference voltage in 20 ms (Fig. 6(a)), while the other methods arrive with delay and present large oscillations in every variation of insolation and temperature. However when the partial shading occur, at 2 s, the method proposed by [13] present a wrong voltage and illustrates the low current among the methods mentioned before, as shown in Fig. 6(b), as results the method InC-BSC fail to tracks the global maximum power point (GMPP) and get stack to a local maximum power point (LMPP) which causes a loss of almost 20 W, as shown in the Fig. 6(c). While the proposed method distinguee the GMPP and tracks it with high performance.

The Fig. 7 illustrates the power at the output of the SEPIC converter. The results are compared to the method mentioned before. It can be seen from the figure, that proposed method exhibits excellent performance as the curve are smooth and react to the brusque variation of temperature and insolation with high precision. It can be noticed that method SLG-BSC presents good performance, as well compared to the PSO-BSC, as this latter suffer from oscillations. However, the method InC-BSC present a loss considerable of power when partial shading occurs, which make it not recommended for maximum power tracking algorithms.

5. Experimental study

5.1 Experimental setup

The proposed PV system consists of two 20 W SP modules connected in series, one of which has been partially shaded, a SEPIC converter, An Arduino board and a resistive load, as shown in Fig. 8.

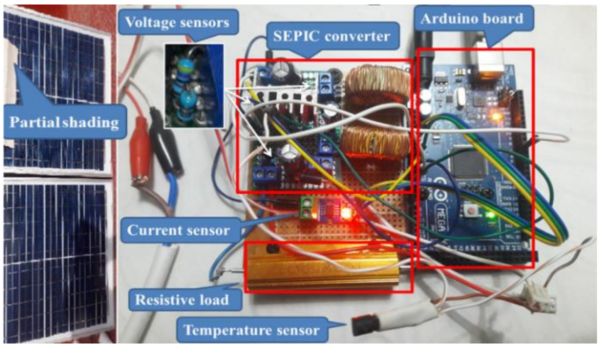

Figure. 8 Experimental setup

The proposed maximum power point tracking algorithm tracks the reference voltage given by the ANN, which is based on actual temperature and current values. Moreover the voltage of the panel as well as the voltage of the second capacitor and the voltage at the output of the converter must be measured.

5.1.1. Voltage sensors:

The commercial voltage sensors are made by using two resistances as shown in figure 8, thus six resistances of 6 Ω and 47 Ω has been implemented in the converter to measure the voltage across the panel, the second capacitor and at the output of the converter, using the voltage divider method.

5.1.2. Current sensor

In order to measure the photovoltaic current, the ACS712 sensor has been used, it uses the Hall effect which detects the magnetic field produced by the induction of the current passing through the measured string.

5.1.3. Temperature sensor

The LM35 sensor was used because it is more accurate than the thermistor and does not require calibration. The temperature is calculated on the basis that its output voltage increases by 0.01 volts for each degree of Celsius temperature.

The datasheet parameters, the extracted parameters extracted from the SP 20W module as well as the SEPIC parameters are shown in Table 4, 5 and 6 respectively.

Table 4. Datasheet of the module SUNRO 20 W

Parameters	Values
V_m (V)	17.3
I_m (A)	1.16
V_{co} (V)	21.7
I_{cc} (A)	1.26
K_i (A /K)	$0.35.10^{-3}$
K_v (V/K)	-0.100

Received: May 8, 2022. Revised: June 14, 2022.

Table 5. Extracted parameters of the module SP 20 W

Parameters	Values
a_1	0.9998
a_2	2.0002
I_{ph} (A)	1.2625
I_{01} (A)	$7.1494.10^{-11}$
I_{02} (A)	$9.9842.10^{-07}$
R_p (Ω)	647.5321
R_s (Ω)	1.2873

Table 6. Components of the SEPIC converter

Parameters	values
DIODE	Schottky SR-450
MOSFET	IRLZ44.
L_1 (mH)	1
L_2(mH)	1
C_1(µF)	1000
C_2(µF)	200
C_3(µF)	1000

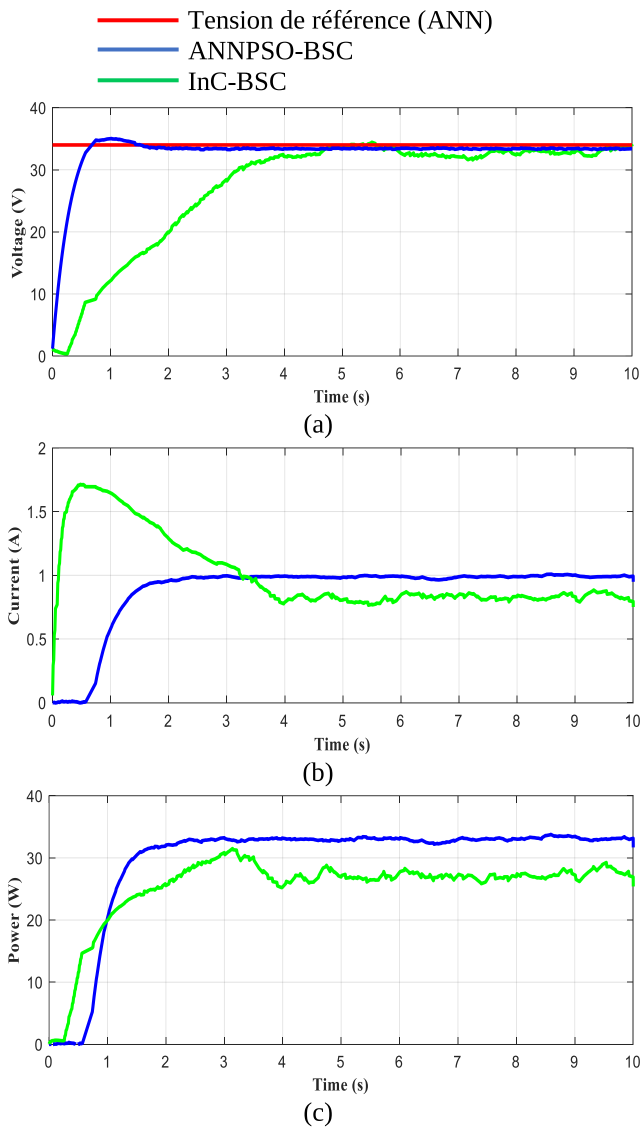

Figure. 9 Photovoltaic: (a) Voltage, (b) Current, and (c) Power

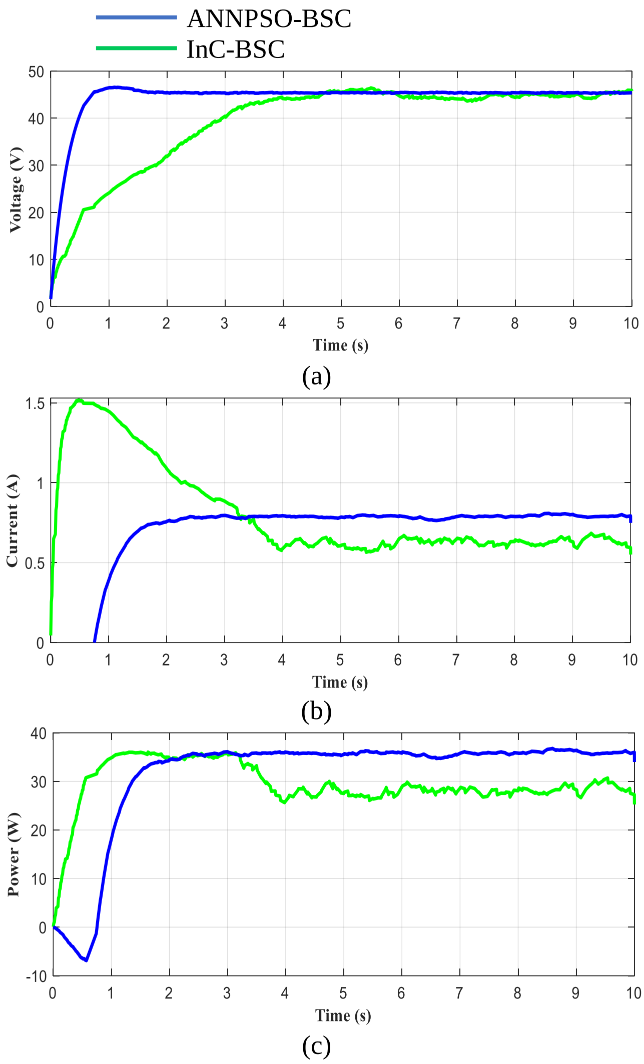

Figure. 10 Output: (a) Voltage, (b) Current, and (c) Power

5.2 Experimental results

The Fig. 9 shows the voltage, current and power of SP20W photovoltaic module during partial shading, obtained by ANNPSO-BSC and InC-BSC commands. Fig. 9(a) shows that the drive successfully tracked the reference voltage in about 0.5 s, while the InC-BSC drive exhibits slow response time and is characterized by large oscillations. Regarding the current (Fig. 9(b)), the ANNPSO-BSC command generates a current of the order of 1 A instead of 1.16 A, mentioned in the data sheet of each PV module. This decrease in current is due to partial shading. The InC-BSC command has a greater decrease since it can generate only 0.7 A. Analysis of Fig. 9(c) shows that the InC-BSC command fails to follow the global maximum power point (GPPM) and locks in the local maximum power point (LPPM), which leads to a power drop of about 13 Watt for the InC-BSC control against only 8 Watt for the ANNPSO-BSC control.

 DOI: 10.22266/ijies2022.0831.49

The Fig. 10 illustrates the voltage, current and power at the terminals of a resistive load under the effect of non-uniform insolation, obtained by the ANNPSO-BSC and InC-BSC commands. Fig. 10(a) shows that the proposed method guarantees a stable voltage with a much faster response time compared to the InC-BSC method. The analysis of Fig. 10(b) shows that when using the proposed control, the load is supplied by a stable current whose amplitude greatly exceeds that of the InC-BSC control. Regarding the power available to the load, the ANNPSO-BSC control guarantees a high and stable power compared to the InC-BSC method.

6. Conclusion:

In this article, an improved MPPT controller for uniform and non-uniform insolation was presented. The proposed approach consists of an artificial neural network, based particle swarm optimization, combined with the backstepping controller. The proposed approach relies on the abality of the PSO algorithm to locate and track the global maximum power point and on the ANN to generate a fast and stable reference voltage. The BSC was introduced to track the reference voltage by adjusting the SEPIC converter. The present technic was simulated in the Matlab/Simulink environment as well as the SLG-BSC, PSO-BSC and InC-BSC techniques. On the one hand, the results show the ability of the proposed technique to follow the GMPP and gain more power, while the InC-BSC technique illustrates a loss of almost 20 W, since it track only the LMPP. On the other hand, the simulation confirms the superiority of the proposed method over the SLG-BSC and PSO-BSC techniques, as it tracks the reference voltage in only 20 ms and exhibits a fast and stable response when the environmental conditions change, while other methods suffer from delays and fluctuations. Moreover, the experimental study confirms the performance of the proposed approach in the real outdoor conditions, as it represents a gain of 5 W and a fast and stable response against the InC-BSC control.

Conflicts of Interest

The authors declare no conflict of interest.

Author Contributions

Khalid Chennoufi has designed, simulated and implemented the proposed approach. Mohammed Ferfra studied the design, validated the results and supervised the experimental study. Hicham Bouzakri contributed to the editing and writing of the manuscript. All authors reviewed the results and approved the final version of the manuscript.

References

[1] R. E. Idrissi, A. Abbou, M. Mokhlis, H. Bouzakri, and Y. E. Houm, "Real-Time Implementation of a PV System Maximum Power Point Tracking Based on the ANN-Backstepping Sliding Mode Control", *International Journal of Renewable Energy Research*, Vol. 11, pp. 1959-1967, 2021.

[2] D. P. Winston, S. Kumaravel, B. P. Kumar, and D. Barkaran, "Performance improvement of solar PV array topologies during various partial shading conditions", *Solar Energy*, Vol. 196, pp. 228-242, 2020.

[3] A. K. Abdelsalam, A. M. Massoud, S. Ahmed, and P. N. Enjeti, "High-performance adaptive Perturb and observe MPPT technique for photovoltaic-based microgrids", *IEEE Transactions on Power Electronics*, Vol. 26, No. 4, pp. 1010-1021, 2011.

[4] Y. Hu, W. Xu, and J. Zhu, "Photovoltaic maximum power tracking control based on modified variable step conductance increment method", *Electrical Engineering*, Vol. 20, No. 3, pp. 29-34, 2019.

[5] J. Ahmad, "A fractional open circuit voltage based maximum power point tracker for photovoltaic arrays", In: *Proc. of the 2nd International Conference on Software Technology and Engineering*, Vol. 1, pp. V1-247-V1-250, 2010.

[6] A. Bellini, S. Bifaretti, and V. Iacovone, "MPPT algorithm for current balancing of partially shaded photovoltaic modules", In: *Proc. of IEEE International Symposium on Industrial Electronics*, pp. 933-938, 2010.

[7] O. Zebraoui and M. Bouzi, "Robust sliding mode control based MPPT for a PV/Wind hybrid energy system", *International Journal of Intelligent Engineering and Systems*, Vol. 11, No. 5, pp. 290-300, 2018, doi: 10.22266/ijies2018.1031.27.

[8] A. Taouni, A. Abbou, M. Akherraz, A. Ouchatti, and R. Majdoul, "MPPT design for photovoltaic system using backstepping control with boost converter", In: *Proc. of International Renewable and Sustainable Energy Conference*, pp. 469- 475, 2016.

[9] K. Ishaque and Z. Salam, "A deterministic particle swarm optimization maximum power point tracker for photovoltaic system under

partial shading condition", *IEEE Transactions on Industrial Electronics*, Vol. 60, No. 8, pp. 3195-3206, 2013.

[10] R. Storn and K. Price, "Minimizing the real functions of the ICEC'96 contest by differential evolution", In: *Proc. of The IEEE International Conference on Evolutionary Computation*, pp. 842-844, 1996.

[11] C. C. Ahmed, M. Cherkaoui, M. Mokhlis, and M. Bahij, "Genetic Algorithm and Backstepping Controller for Photovoltaic System under Partial Shading Effect", *International Journal of Renewable Energy Research*, Vol. 11, No. 1, pp. 83-91, 2021.

[12] A. A. Kamil, M. S. Nasr, and S. Alwash, "Maximum Power Point Tracking Method for Photovoltaic System Based on Enhanced Particle Swarm Optimization Algorithm Under Partial Shading Condition", *International Journal of Intelligent Engineering and Systems*, Vol. 13, No. 6, 2020, doi: 10.22266/ijies2020.1231.22.

[13] C. C. Ahmed, M. Cherkaoui, and M. Mokhlis, "PSO-SMC Controller Based GMPPT Technique for Photovoltaic Panel Under Partial Shading Effect", *International Journal of Intelligent Engineering and Systems*, Vol. 13, No. 2, pp. 307-316, 2020, doi: 10.22266/ijies2020.0430.30.

[14] M. Mokhlis, M. Ferfra, A. Abbou, and R. E. Idrissi, "Robust Control for Photovoltaic System Under Partial Shading Effect Using the SEPIC Converter", *International Journal of Renewable Energy Research*, Vol. 9, No. 2, pp. 684-691, 2019.

[15] K. Chennoufi, M. Ferfra, and M. Mokhlis, "Design and Implementation of Efficient MPPT Controllers based on SDM and DDM using Backstepping Control and SEPIC Converter", In: *Proc. of 9th International Renewable and Sustainable Energy Conference*, pp. 1-8, 2021.

[16] R. W. Erickson and D. Maksimovic, "Fundamentals of Power Electronics", *Springer Science & Business Media*, 2007.

[17] K. Chennoufi and M.Ferfra, "Maximum Power Point Tracking using SEPIC converter and double diode solar cell model", In: *Proc. of International Conference on Digital Technologies and Applications*, pp. 1159-1169, 2021.

[18] K. Chennoufi and M. Ferfra, "Parameters extraction of photovoltaic modules using a combined analytical - numerical method", In: *Proc. of International Conference on Cloud Computing Technologies and Applications*, pp. 1-7, 2020

[19] K. Chennoufi, M. Ferfra, and M. Mokhlis, "An accurate modelling of Photovoltaic modules based on two-diode model", *Renewable Energy*, Vol. 167, pp. 294-305, 2021.

[20] L. V. Fausett, "Fundamentals of neural networks: architectures, algorithms and applications Fundamentals of neural networks: architectures, algorithms and applications", *Pearson Education India*, 2006.

[21] D. Merkle and M. M., *Swarm Intelligence*, Book Chapter 14, p. 37.

[22] V. Phimmasone, K. Kondo, T. Kamejima, and M. Miyatake, "Evaluation of extracted energy from PV with PSO-based MPPT against various types of solar irradiation changes", In: *Proc. of International Conference on Electrical Machines and Systems*, pp. 487-492, 2010.